

Subwavelength Confinement in Integrated Metal Slot Waveguide on Silicon

Long Chen, Jagat Shakya, Michal Lipson

School of Electrical and Computer Engineering, Cornell University, Ithaca, NY 14853

Abstract: We demonstrate propagation losses of less than $0.8 \text{ dB}/\mu\text{m}$ in a metal slot waveguide on silicon with predicted confinement substantially below the optical wavelength ($\sim 1.55 \mu\text{m}$). We also show compact and efficient coupling of the high confinement metal slot waveguide with a standard silicon dielectric waveguide with coupling efficiency of approximately 2.5 dB per facet.

©2006 Optical Society of America

OCIS codes: (130.3120) Integrated optics devices; (240.6680) Surface plasmons

There is a growing research interest in optical circuits at the nanometer scale for future integration of optical, optoelectronic and electronic devices on chip. For this goal, however, the typical dimensions of conventional dielectric waveguides are dictated by diffraction, therefore limiting dense on-chip integration. Plasmonic waveguides such as nanoparticle chains [1], nanorods [2], in contrast, guide light through the interaction of photon and electron oscillation around the metal surface, and are potential candidates for nanoscale optical elements with sizes much smaller than the diffraction limit. The tradeoff between the confinement level and

propagation loss, however, is a fundamental limitation of such waveguides. For example, for visible light, nanoparticle chains with confinement of approximately $\lambda/5$ have been reported with propagation loss of $30 \text{ dB}/\mu\text{m}$ [1]. Therefore, structures offering both high confinement and relatively low loss are desired. Here we demonstrate a low loss plasmonic waveguide with predicted confinement substantially below the optical wavelength ($\sim 1.55 \mu\text{m}$). We also demonstrate efficient integration of the plasmonic waveguide with dielectric silicon wire waveguides.

In order to overcome the traditional limitations of plasmonic waveguides [3], we use the inverted metal slot waveguide with a dielectric core sandwiched between metal cladding [4]. As is general for surface plasmon, the electric field polarized perpendicular to the metal-dielectric interface is bound around the interfaces due to the high dielectric discontinuity between metal and dielectric. When the two interfaces of the metal slot are brought closer together, the plasmonic waves around the two interfaces interact and result in a symmetrical mode where the light is almost completely confined in the dielectric slot, enabling extreme subwavelength confinement across the slot far beyond the diffraction limit. The effective index of the slot increases due to the coupled plasmonic waves [5]. Therefore, for three-dimensional realistic structures the light is vertically confined via the index confinement mechanism. Confinement along this direction can also be significantly below the optical wavelength since the effective index of the slot increases rapidly for very narrow slot. Several two- or three-dimensional structures based on the idea of metal slots have been theoretically analyzed [6-7]. Devices like bends, splitters, Bragg reflectors and nanocavities have been proposed [8,9]. Interferometers and ring resonators based on channel plasmon waveguide [10], which can be interpreted as a metal slot waveguide with vertically tapering width, have been demonstrated very recently [11].

Experimental guiding through a slot in a thin metal film has been reported [12], and efficient coupling of a metal slot with a micron size dielectric slab waveguide has also been recently predicted [13]. Here we show experimentally a low loss metal/dielectric waveguide on silicon substrate with predicted high confinement for infrared propagation. We measure for the first time the propagation losses of such waveguides. We also show for the first time experimentally high coupling efficiency between these waveguides and dielectric silicon waveguides using very compact tapers. The metal slot waveguide considered here is shown in Fig. 1(a). It consists of a silicon wire cladded by gold which in turn is embedded in silicon dioxide. Silicon is used as the slot due to its high refractive index and more importantly, the convenient integration with silicon wire waveguides. A thin layer of silicon dioxide (~ 80 nm) on top of the silicon isolates the field from the gold on the top. We calculate the eigenmodes and propagation loss of this structure using a full-vectorial finite-difference mode solver [14]. For $\lambda = 1550$ nm, a typical mode profile ($|E_x|$) for a slot dimension of 150-nm-wide and 250-nm-thick is shown in Fig. 1(b), which shows a high lateral confinement of the mode to a region of ~ 150 nm. Since the lateral guiding mechanism is based on coupled surface plasmon instead of interference effect as general in pure dielectric waveguides, similar mode profile remains even when the slot width shrinks down to tens of nanometers. For a 150-nm slot, we calculate the loss due to absorption in the gold to be ~ 0.5 dB/ μm ; for a 50-nm slot, it increases to ~ 1.2 dB/ μm . This is at least one order of magnitude lower than what has been previously demonstrated with similar level of lateral confinement in the nanoparticle chains [1].

In order to integrate the slot waveguide with standard dielectric silicon wire waveguide of 450 nm x 250 nm, we use a compact linear taper to couple light in and out of the metal slot, see

Fig. 2(a). There are three sources of loss in the taper: reflection at the metal/dielectric interface; propagation loss due to absorption in the metal; and reflection and radiation losses due to the tapering. Due to the high confinement of light in the input silicon wire waveguide, the interface reflection is less than 5%. The propagation loss through the taper could be estimated from the dependence of the loss coefficient on the slot width, and monotonously increases with the taper length. However, for very sharp tapers, the tapering loss (due to reflection and radiation) dominates and the overall coupling efficiency decreases. Therefore an optimal taper length exists due to the tradeoff between these two factors. We simulated the input coupling using three dimensional finite-difference time-domain (FDTD) for various taper lengths in the case of 150 nm slot width (see Fig. 2(c)). The E_x field distributions for three couplers of different lengths ($L_t = 325$ nm, 450 nm, 575 nm) as marked by the arrows in Fig. 2(c) are plotted in Fig. 2(d). One can see that for very short tapers ($L_t < 300$ nm), the coupling efficiency drops rapidly. This is the taper dimensions in which the tapering losses dominate. For long tapers ($L_t > 1.5 \mu\text{m}$), the loss due to the tapering is negligible while the propagation loss due to absorption along the taper determines the coupling efficiency. Over this region we find a linear drop in the coupling efficiency. The most efficient coupling with approximately 0.5 dB coupling loss is obtained using $L_t \sim 325$ nm. In the range of maximum coupling efficiency one can see damping with the taper length. These oscillations are due to weak Fabry-Perot (FP) resonances inside the taper with a periodicity of ~ 225 nm consistent with the calculated FP resonance period using $L_{FP} = \lambda / 2n_{eff}$, where $n_{eff} \sim 3.4$ is effective index of the medium estimated from the mode analysis. Note that in the case of zero taper length (direct connection of the 450nm wide silicon wire waveguide with the 150-nm slot) the coupling efficiency is 1.7 dB ($\sim 68\%$ in power). This is because in the eigenmode of the 450-nm-wide silicon wire waveguide, the central 150-nm-wide

region has ~55% of the total power, which results in the high coupling efficiency. For a much narrower slot, e.g., 50-nm slot, the power confined in the central 50-nm-wide region is only ~20% resulting in a coupling efficiency of 3.6 dB when no taper exists. With a similar compact linear taper, the coupling efficiency could be boosted up to 0.7 dB. Note that as shown in the inset of Fig. 2(b), the field is enhanced in the narrow slot region after the taper due to a focusing effect of the plasmonic waves similar to those in metal tips [15] and grooves [16].

We fabricated the metal slot waveguide on a silicon-on-insulator (SOI) wafer with a silicon layer of 250 nm by E-beam lithography patterning, followed by reactive ion etching. The exposed E-beam resist acts as a thin layer of oxide for isolating. A photolithography step was then used with a bi-layer photoresist structure to open the device window for metal evaporation. Note here that in order to allow for misalignment tolerances in the photolithography step, we used a longer taper ($\sim 4 \mu\text{m}$) than the optimal case, for which the coupling efficiency drops to about 2 dB estimated from the propagation loss. During the evaporation the sample stage was slightly tilted and rotated to ensure close contact of the metal with the sidewalls of the silicon wire. After the lift-off process, the whole chip was covered with silicon dioxide through E-beam evaporation. A microscope image of the device region is shown in Fig. 2(b).

Experimentally, we coupled polarized laser light at $\lambda = 1550 \text{ nm}$ from a tapered lens fiber to the silicon wire waveguides terminated with nanotapers [17] and measured the transmitted power using an infrared detector. Fig. 3(a) shows a typical plot of the normalized power versus the length of the metal slot waveguide for a slot width of 150 nm. The transmitted power is normalized to a reference dielectric waveguide with no metal slot therefore the normalization

gives the loss due to the devices. From the linear fit, we find the propagation and the coupling loss for the 150-nm-wide slot to be about $0.8\text{ dB}/\mu\text{m}$ and $\sim 2.5\text{ dB}$ per facet, respectively, both values close to the theoretical predictions. In Fig. 3(b) we show the measured propagation loss of different slot width compared to the simulation results demonstrating a relatively good agreement between the two. The 150-nm slot is the narrowest device we fabricated. For an even narrower slot, e.g., 50 nm, we expect the loss to be $2\sim 3\text{ dB}/\mu\text{m}$. This loss level is at least one order of magnitude lower than what has been previously demonstrated with comparable degree of lateral confinement.

In conclusion, we show a metal slot waveguide with deep subwavelength confinement and propagation loss that is one order of magnitude lower than previously demonstrated with comparable degree of lateral confinement. With a compact taper of about $4\mu\text{m}$ long, we also demonstrate integration of the metal slot and silicon wire with high coupling efficiency of about 2.5 dB per facet. Using an optimal taper length of less than $0.5\mu\text{m}$, the coupling loss is expected to be reduced to about 0.5 dB . The realization of deep subwavelength confinement and efficient coupling with standard dielectric silicon waveguides has attractive applications in nanoscale circuits and on-chip integration of optical, optoelectronic and electronic devices.

The authors acknowledge Christina Manolatu for her assistance in the simulations. This work was supported by the Science and Technology Centers program of the National Science Foundation (NSF) under agreement DMR-0120967, the Semiconductor Research Corporation under Grant No. 2005-RJ-1296, the Cornell Center for Nanoscale Systems, the Cornell Center for Material Research, and the National Science Foundation's CAREER Grant No. 0446571. The

authors would also like to thank Gernot Pomrenke from the Air Force Office of Scientific Research for supporting the work under Grants No. F49620-03-1-0424 and No. FA9550-05-C-0102. This work was performed in part at the Cornell Nanoscale Science & Technology Facility, a member of the National Nanotechnology Infrastructure Network, which is supported by the National Science Foundation under grant ECS-9731293, its users, Cornell University, and industrial affiliates. M. Lipson's e-mail address is lipson@ece.cornell.edu.

Published by

1. S. A. Maier, P. G. Kik, H. A. Atwater, S. Meltzer, E. Harel, B. E. Koel, and A. A.G. Requicha, *Nature Mater.* **2**, 229-232 (2003)
2. J. Takahara, S. Yamaguchi, H. Taki, A. Morimoto, and T. Kobayashi, *Opt. Lett.* **22**, 475 (1997)
3. J. C. Weeber, Y. Lacroute, and A. Dereux, *Phys. Rev. B* **68**, 115401 (2003)
4. R. Zia, M. D. Selker, P. B. Catrysse, and M. L. Brongersma, *J. Opt. Soc. Am. A* **21**, 2442 (2004)
5. K. Tanaka and M. Tanaka, *Appl. Phys. Lett.* **82**, 1158 (2005)
6. L. Liu, Z. Han, and S. He, *Opt. Express* **13**, 6645 (2005)
7. G. Veronis and S. Fan, *Opt. Lett.* **30**, 3359 (2005)
8. G. Veronis and S. Fan, *Appl. Phys. Lett.* **87**, 131102 (2005)
9. B. Wang and G. Wang, *Appl. Phys. Lett.* **87**, 013107 (2005)
10. S. I. Bozhevolnyi, V. S. Volkov, E. Devaux, and T. W. Ebbesen, *Phys. Rev. Lett.* **95**, 046802 (2005)

11. S. I. Bozhevolnyi, V. S. Volkov, E. Devaux, J. Laluet, and T. W. Ebbesen, *Nature* **440**, 508 (2006)
12. D. F. P. Pile, T. Ogawa, D. K. Gramotnev, Y. Matsuzaki, K. C. Vernon, K. Yamaguchi, T. Okamoto, M. Haraguchi, and M. Fukui, *Appl. Phys. Lett.* **87**, 261114 (2005)
13. P. Ginzburg, D. Arbel, and M. Orenstein, *CLEO CWN5* (2005)
14. C. L. Xu, W. P. Huang, M. S. Stern, and S. K. Chaudhuri, *IEE Proc. Optoelectron.* **141**, 281 (1994)
15. M. I. Stockman, *Phys. Rev. Lett.* **93**, 137404 (2004)
16. D. K. Gramotnev, *J. Appl. Phys.* **98**, 104302 (2005)
17. V. R. Almeida, R. R. Panepucci, and M. Lipson, *Opt. Lett.* **28**, 1302 (2003)

Published by
OSA

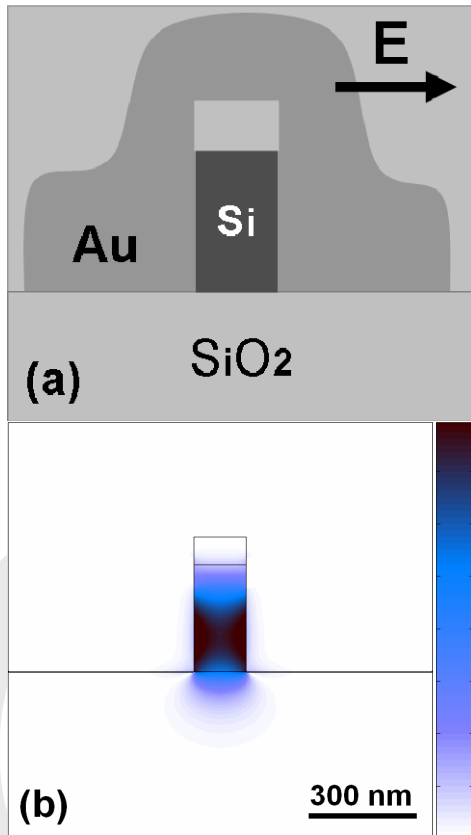


Fig. 1 (color online): Schematics (a) and $|E_x|$ mode profile (b) of the metal slot waveguide with a 150-nm-wide silicon core.

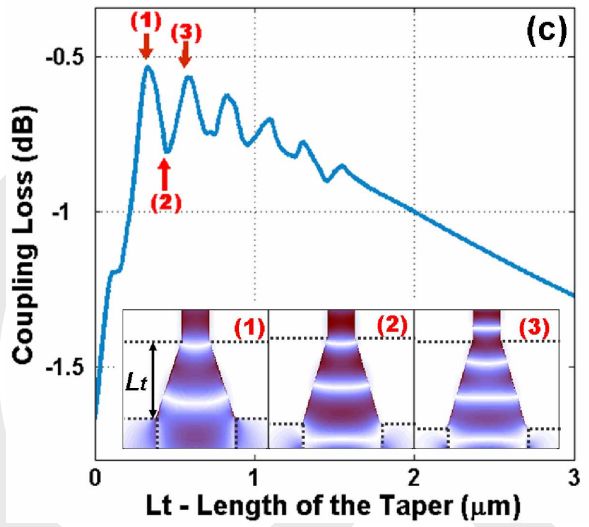
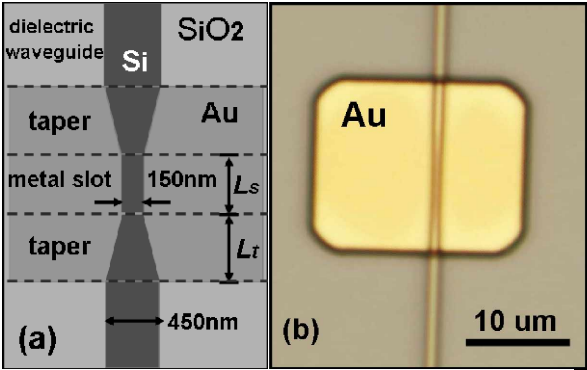


Fig. 2 (color online): Schematic (a) and microscope image (b) of the metal slot integrated with a dielectric silicon wire waveguide; (c) FDTD simulation of the coupling loss versus the taper length for the 150-nm-wide slot. Inset: E_x field distribution of the taper coupler for various taper lengths as indicated by the arrows: (1) $L_t=325$ nm, (2) 450 nm and (3) 575 nm respectively.

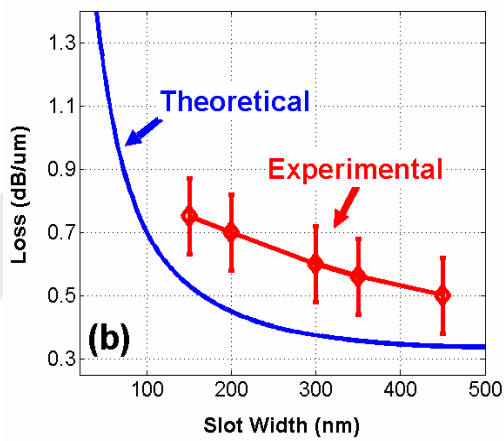
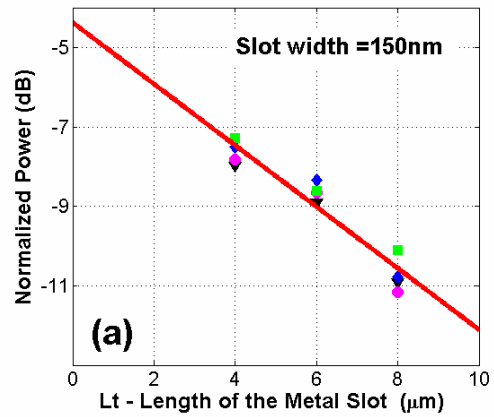


Fig. 3: (a) Normalized transmitted power versus length of the metal slot waveguide for a slot width of 150 nm; (b) theoretical and experimental propagation losses for several slot waveguides with different slot width.